Vol. 14, No. 39, Summer 2024, pages 27-45

Journal of Analytical and Numerical Methods in Mining Engineering

Journal home page: http://anm.yazd.ac.ir/

Research article

Evaluation of Tunnel Boring Machine (TBM) Based on Different Cutting Tool Layouts in the Cutter-Head

Mohsen Alebouyeh[1], Majid Noorian-Bidgoli[1]*, Ali Aalianvari[1]

1- Dept. of Mining Engineering, Faculty of Engineering, University of Kashan, Kashan, Iran

*Corresponding author: E-mail: *noriyan@kashanu.ac.ir*

(Received: *November 2023*, Accepted: *June 2024)*

DOI: 10.22034/ANM.2024.20911.1616

Keywords

Tunnel Boring Machine (TBM)

Machine learning modeling

Stochastic layout

Star layout

Spiral layout

GWO algorithm

Abstract

The arrangement and layout of cutting tools in the cutter head are among the most critical factors affecting the performance of the Tunnel Boring Machine (TBM). These factors directly impact the drilling operation efficiency, the TBM's useful lifespan, and the cutting tool's overall performance. In general, designing the cutting tool layout poses a multi-objective optimization challenge with non-linear constraints, resulting in computational complexity during the design process. Researchers have faced significant challenges in developing efficient computational models for designing cutting tool layouts in TBMs due to the complexities arising from the technical requirements of TBM structures and drilling engineering constraints. In this study, the primary aim is to assess the influence of different cutting tool layouts on TBM performance. To achieve this, a numerical model has been created, employing the Grey Wolf Optimization (GWO) metaheuristic algorithm to design three types of layouts: stochastic, spiral, and star. To evaluate the performance of the developed design model, a practical TBM for rock excavation was selected, and the process of designing the cutting tool layout in its cutter head was analyzed. According to the research findings, it is evident that the TBM's performance has shown remarkable improvement with all three types of cutting tool layouts: stochastic, spiral, and star, compared to the original setup. The results indicate that the TBM with a stochastic cutting tool layout outperformed the spiral and star layouts, achieving an approximately 8% reduction in the overall lateral force compared to the star layout, and a 10% reduction compared to the spiral layout. Furthermore, the stochastic layouts led to an 11% decrease in eccentric torque compared to the star layout, and a 14% decrease compared to the spiral layout. After analyzing the results and assessing the TBM's performance under the spiral and star layouts, it was evident that the TBM with the star cutting tool layout outperformed the spiral layouts. The star layout resulted in a more significant reduction, approximately 4%, in the overall lateral force of the TBM and a 2.5% decrease in the eccentric torque compared to the spiral layouts. The most crucial outcome of this research was the successful development of an efficient numerical model for designing optimal cutting tool layouts, including stochastic, spiral, and star layouts in the TBM cutter head, utilizing the GWO algorithm. The proposed model exhibited versatility, making it applicable to different operational conditions and various types of TBMs.

1. INTRODUCTION

The mechanized TBMs represent modern engineering achievements for excavating underground spaces, serving various purposes such as road construction, water and power transmission tunnels, railway networks, etc. TBMs come in diverse types, selected based on specific project requirements, which include environmental factors like soil properties, rock

characteristics, varying working face conditions, and groundwater levels. These mechanized machines consist of multiple components, each contributing to their unique structural complexities. These mechanized TBMs are highly expensive, and their deployment in different projects necessitates thorough evaluation and precise performance assessment. Mechanized TBM excavation offers several advantages, including automated and mechanized drilling, and reduced noise and vibrations compared to blasting techniques, making it a prominent achievement in the field of drilling engineering. Today, mechanized tunneling and the use of TBMs are widely adopted as a suitable alternative to conventional tunneling in various regions around the world (Yu, 2007; Cho et al., 2008; Jeong et al., 2011; Choi and Lee, 2015). The utilization of TBMs, the time and cost of tunnel drilling, particularly in hard rock conditions, are influenced by three key parameters: 1) Rock properties (including rock abrasivity and the rock mass portability), 2) TBM parameters (such as the drilling power specifications of the TBM), 3) The design of the cutter-head in the TBM (Yu, 2007).

When drilling through hard rock using TBMs, the consumption of cutter discs becomes a crucial aspect that demands careful consideration, as it constitutes at least 10% of the total drilling costs (Bruland, 2000). The cutter head, positioned at the forefront of the TBM, directly interacts with the tunnel surface (working face) making it a key factor in the efficiency of tunnel drilling. It significantly influences the TBM's productivity, drilling speed, operational reliability, and stability (Zhang, 2009; Zhao-Huang and Yong, 2011; Sun et al., 2018). Previous extensive research and empirical evidence from the performance of TBMs in hard rock conditions indicate a strong connection between drilling costs and the TBM's overall efficiency (Alber et al., 2014, Macias et al. 2015, Wang et al. 2015). Moreover, studies (e.g., Macias 2016) emphasize that the design of the cutter-head layout stands as the primary component in enhancing the TBM's efficiency for cutting through hard rock.

The design of the cutter-head in a TBM involves two essential aspects: the structure design of the disc body (cutting tools) and the design of the cutting tools layout. In general, irrespective of the type of mechanized tunnel boring machine, the cutter-head comprises five main components, including 1) Normal Cutters, 2) Manhole, 3) Bucket, 4) Center Cutters, and 5) Gauge Cutters. Fig. 1 depicts the cutter head, along with the cutting tools and equipment, in both actual TBM and schematic forms.

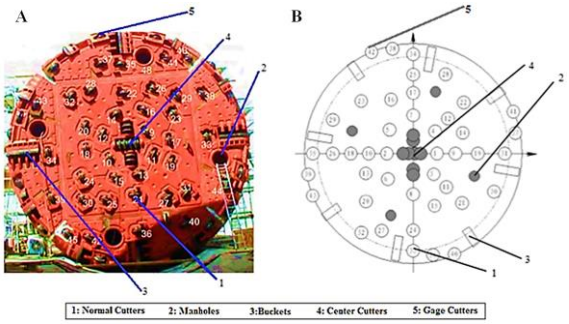

Fig. 1. A general view of the equipment of the TBM cutter-head.

The design of the cutting tool layout in the TBM is closely related to the cutter's penetration into the rock, cutting forces, and the machine's expected performance. During drilling, three cutting forces are exerted on the tip of the disc cutter: normal force, rolling force, and lateral force. Fig. 2 schematically illustrates the forces acting on the normal and gauge cutters.

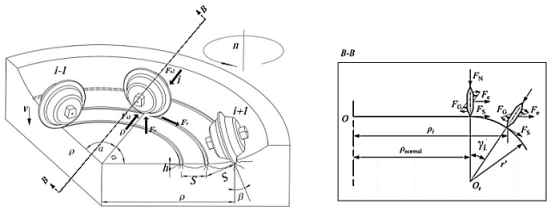

Fig. 2. Schematic of forces acting on normal and gauge cutters.

The design process of the cutting tool layout in the TBM cutter-head emphasizes two main principles: 1) Enhancing drilling efficiency and establishing the ideal technical conditions for the TBM's performance (engineering technical requirements), 2) Ensuring compliance with the design constraints of the cutter-head structure, including the placement of the manhole and bucket, as well as ensuring the required strength of the equipment (structural design requirements). In the design of the cutting tool layout for TBMs, encountering a multi-objective optimization problem with non-linear constraints leads to computational complexity during the design process. The primary objective is to achieve a balanced distribution of forces on the cutter-head during drilling. In other words, the optimal design of the cutting tools layout aims to minimize the eccentric forces and moments, creating an ideal state for the cutting tools and their supports. However, due to complex engineering technical requirements, the nature of the rock at the working face, and design constraints, it is not always possible to eliminate eccentric forces and moments. Therefore, studying the disc cutter layout in TBMs becomes crucial to address these challenges, improve the cutting tool's performance, and cutter's useful

lifespan, enhance the overall TBM efficiency, and ultimately reduce tunnel drilling costs (Huo et al., 2011b).

The design of the cutting tool layout in the TBM cutter head involves two primary stages: 1) Designing the cutting spacing parameter (S), and 2) Designing the layout of the normal and gauge cutters. In the first stage (designing the cutting spacing), researchers have conducted numerous numerical (Gong et al., 2005, 2006a, b) and laboratory experiments (Moon, 2006; Abu Bakar et al., 2014; Cardu et al., 2017).

Utilizing a linear cutting machine (LCM) and considering the physical and mechanical properties of the hard rock being tested, the cutting spacing is calculated. After determining the cutting spacing, and the design of the cutting tool layout, several different requirements must be considered. Meeting all these conditions adds to the complexity of the problem and presents one of the significant challenges faced by researchers. It is important to note that the cutting spacing design was not the focus of this research, and the primary objective was to determine the optimal layout of the cutting tools. After determining the cutting spacing for the disc cutters, the subsequent step involves implementing the design of the cutting tool layout in the cutter head. In the design of the disc cutter layout, numerous technical and engineering requirements, as well as structural design constraints of the cutter head, need to be met. The engineering requirements involve minimizing eccentric forces, eccentric torque of the cutter-head, and the overlapping region between cutter cuts, and maximizing the number of consecutive cuts between adjacent disc cutters. The structural design constraints of the cutter-head encompass the positioning of buckets and manholes, as well as equipment assembly considerations. All of these requirements create conflicting constraints in the design of the disc cutter layout, which must be taken into account as constraints during the design process.

Until now, relatively comprehensive research has been conducted to assess and design the cutting tool layout in the TBM cutter-head (Gong et al., 2005; Moon, 2006; Huo et al., 2011b, 2006a, b; Zhao-Huang and Yong, 2011; Abu Bakar et al., 2014; Alber et al., 2014; Macias et al., 2015; Wang et al., 2015; Macias, 2016; Sun et al., 2018).

In general, the proposed layouts can be classified into three types: 1- Spiral layout pattern, 2- Star layout pattern, and 3- Stochastic layout pattern. Fig. 3 illustrates these three main types of cutting tool layouts in the TBM cutter head.

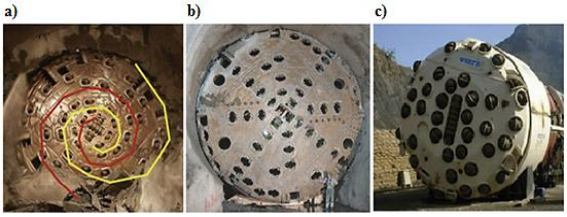

Fig. 3. Different layouts of cutting tools in TBM, (a) Spiral layout, (b) Star layout, (C) Stochastic layout.

Each of the three types of cutting tool layouts has its advantages and disadvantages in terms of evaluating the performance of the TBM machine in excavation operations. The spiral layout is one of the cutting tool layouts employed in the cutter head, where the helical positioning of the normal cutters has resulted in satisfactory TBM performance. The effectiveness of the spiral layout has been thoroughly examined and evaluated in the study conducted by Geng et al. (2018). The spiral layout is further categorized based on the number of helical loops formed in the cutter head, including multi-spiral, 2-spiral, 4-spiral, 6-spiral, and 8-spiral layouts. Fig. 3 (a) illustrates the multi-spiral type, and in Fig. 4, a schematic representation of various spiral layouts is displayed.

The star layout (Fig. 3(b)), also referred to as the Spoke layout in some sources, is one of the cutting tool layouts used in the cutter head. It derives its name from the arrangement of the normal cutters, resembling the spokes of a star. The satisfactory performance of the star layout has been evaluated and studied in research conducted by Huo et al. (2011b) and Geng et al. (2018).

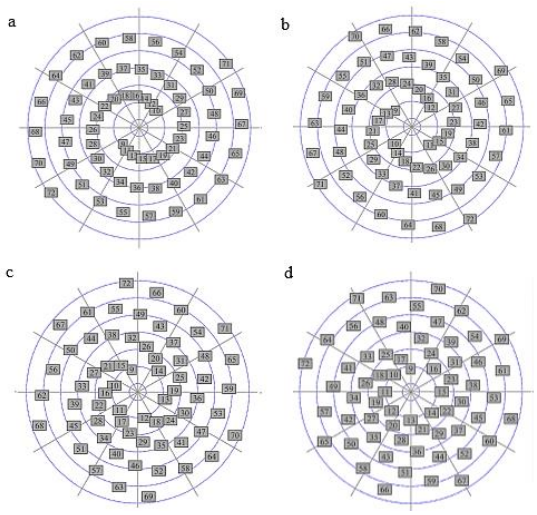

Fig. 4. Schematic of various types of spiral cutting tool layouts. (a) 2-Spiral, (b) 4-Spiral, (c) 6-Spiral, (d) 8-Spiral (Gong et al., 2006b).

The star layout is further classified based on the number of spokes (branches of the star) in the cutter head, with two of the most commonly

utilized layouts being the 8-spoke star layout and the 12-spoke star layout. Fig. 5 illustrates a schematic representation of various star layouts.

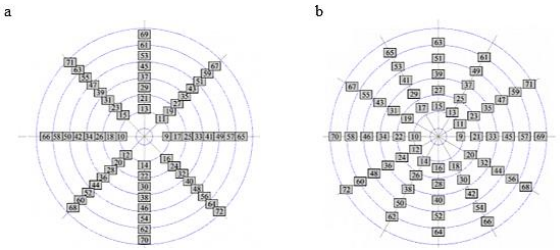

Fig. 5. Schematic of various types of star-cutting tool layouts. (a) 8-Spoke Star, (b) 12-Spoke Star.

Researchers have conducted various studies on the design of cutting tool layouts in TBMs. Cigla et al. (2001) introduced the CSM computer model, which utilizes semi-empirical equations to estimate cutting forces in the design of TBMs for hard rock, taking into account cutter-head specifications and rock properties. Rostami (2008) explored modeling methods for the cutter head of hard rock TBMs. The proposed model, based on estimating cutting forces, has proven effective in optimizing cutter head design and predicting TBM performance. Huo et al. (2011a) conducted a comprehensive investigation and evaluation of optimal cutting tool layouts in the cutter head of TBM for different layouts. To achieve this, they employed a genetic algorithm to optimize the positioning and design of the cutting tools.

Several studies have been dedicated to assessing optimization methods for cutting tool layouts in the TBM cutter head, including works by Sun et al. (2013); Huo et al. (2015); Mazaira and Konicek (2015); and Liang et al. (2016).

Geng et al. (2018) extensively studied various types of cutting tool layouts in TBM cutter heads. Their research findings provided valuable insights into the pros and cons of different layouts during practical excavation operations. Additionally, they proposed criteria for optimizing different parameter settings in the cutting tool layouts. Sun et al. (2018) conducted a thorough investigation into the design of cutting tool layouts for TBM. They focused on analyzing the structural aspects of the TBM cutter head and provided a relatively comprehensive formulation for the design process, considering both structural and engineering requirements in detail. Lin et al. (2019) evaluated the cutting tool layout in TBMs, taking into account various parameters such as rock-breaking capability, energy consumption, load-bearing capacity, and the useful lifespan of the disc cutter. In these studies, a multi-objective optimization model was developed to determine the optimal layout of cutting tools.

The researchers employed the Genetic Algorithm (GA) and utilized the Fuzzy Analytical Hierarchy Process (FAHP) to calculate weight coefficients. The findings indicated significant improvements in the TBM's performance for rock cutting and an increased lifespan of the disc cutter after applying the proposed optimization method (Lin et al. 2019). In their research, Yang et al. (2020) focused on evaluating the optimal layout of the cutting equipment in the TBM cutter head. They specifically looked into determining the best positioning for the buckets. The study explored how the number, angular orientation, and spacing of buckets could impact the machine's drilling performance.

In another study, Farrokh (2021) assessed the influence of the cutting tool layout on cutting penetration and proposed a fundamental guideline for optimizing the cutting distance. To achieve this, a comprehensive field database was utilized to examine the effects of different rock types and uniaxial compressive strengths on cutting penetration at various cutter spacing conditions in the cutter head. Studies on the design characteristics of the cutting tool layout in cutter-head have yielded significant findings. Uniformly distributing cutting tools in the cutter head has been shown to enhance drilling efficiency.

Duan et al. (2022) conducted comprehensive research incorporating laboratory experiments and numerical simulations to investigate the impact of cutting tools and their cutting profiles on hard rock excavation. In another study by Liu et al. (2022), a multi-objective optimization approach was employed to control and evaluate the performance of TBMs. The optimization techniques proved effective in improving TBM performance and enhancing control in uncertain conditions. Furthermore, Farrokh (2022) researched to assess various cutting tool layouts in TBMs, examining both star and spiral cutting tool layouts in the cutter head.

Through the examination of previous studies, it becomes evident that optimizing the efficient layout of cutting tools in the TBM's cutter head has been a major challenge for researchers. Numerous investigations have been carried out in this area. Furthermore, computational approaches utilizing advanced optimization algorithms can effectively address engineering layout design problems. Hence, the necessity for developing a practical computational model based on sophisticated computational methods and efficient optimization algorithms to design the cutting tool layout in the TBM's cutter-head stands out as a clear research gap. The Grey Wolf Optimizer (GWO) algorithm,

introduced by Mirjalili et al. (2014), is a type of metaheuristic and population-based optimization algorithm inspired by the hunting behavior of grey wolves. Researchers have extensively demonstrated the effectiveness and remarkable performance of the GWO algorithm in solving various engineering problems (e.g., Emmanuel et al. 2021). The main goal of this research is to assess the influence of three types of layouts, namely stochastic, spiral, and star, on the performance of the TBM. To accomplish this, three distinct models have been developed for designing each of these layouts, employing the GWO algorithm as the optimization technique. To achieve the optimal design model, the research involved evaluating the relationships and equations governing the performance of rock-cutting tools in TBM. All constraints, design requirements, and equations were taken into account during the development of a numerical model for the layout design of disc cutters in the TBM's cutter head. The GWO algorithm was employed for optimization in this model development process. Furthermore, the performance of the developed model was evaluated by examining the cutting tool layout design for an operational TBM prototype.

2. MATERIALS AND METHODS

The primary aim of this study is to propose an optimized model for designing cutting tools with three different layouts (stochastic, spiral, star) in the TBM cutter head, using the GWO optimization algorithm. To achieve this, the requirements and constraints that govern the process of designing the cutting tool layout in the TBM cutter head are examined. The design of cutting tools in the TBM cutter head must consider various technical, engineering, and structural constraints to provide the best possible design. Therefore, evaluating these requirements helps establish the main optimization equation and constraints for the optimal design of the cutting tool layout. The essential design requirements and conditions for the cutting tool layout are presented in Table 1.

Table 1. Requirements and constraints for designing the cutting tool layout in TBM

Classification	Requirements/Constraints	Explanation
Technical-Engineering requirements of drilling	Minimization of eccentric forces	The eccentric forces should be minimized as much as possible.
	Minimization of eccentric torques	The eccentric torques should be minimized as much as possible.
	Minimization of eccentricity error value	The eccentricity error value of the entire system should not exceed the permissible limit, and minimizing it is preferable.
	Constraint of overlapping in cutting	To maintain high cutting efficiency, all adjacent discs should sequentially crush the rock.
Structural constraints of TBM	Constraint of non-overlapping cutter positions	All disc cutters must be located within the cutter head without any overlapping between them.
	Constraint of non-overlapping positions of tools and cutter head equipment	The positions of the cutters must not overlap with the positions of manholes and buckets.

Referring to Table 1, it becomes evident that the key components for formulating the main optimization equation are the minimization of 1- eccentric forces, 2- eccentric torques, and 3- eccentricity error value. Moreover, the optimization constraints should include 1- consecutive cutting, 2- non-overlapping cutter positions, and 3- non-overlapping of cutter head equipment.

2.1. Design Requirements Of Normal And Gauge Cutters

In the process of designing the cutter tool layout for the TBM cutter-head, besides the factors mentioned in Table 1, specific requirements have been encountered for determining the positions of normal and gauge cutters based on their respective functions. The normal cutters serve as the primary tools for cutting hard rock within the cutter head. They achieve rock cutting through rotation and the application of thrust force. On the other hand, the gauge cutters are strategically placed in the transitional zone of the cutter head. Their main role is to maintain tunnel geometry and reduce the vibration of the cutter head. Additionally, the gauge cutters are designed with a deviation angle (γ) relative to the center of the cutter head. For normal cutters, this deviation angle is considered to be zero, and their rotation axis is aligned along the radial direction of the cutter head.

Practical engineering applications reveal that gauge cutters, with their high linear velocity and assembly method (characterized by a deviation angle), are susceptible to damage (Gong et al., 2005, 2006a, b; Moon, 2006; Rostami, 2008; Huo et al., 2011a, b; Abu Bakar et al., 2014; Cardu et al., 2017; Cigla et al., 2018; Geng et al., 2018,).

Based on statistical data and operational experiences, the transitional zone radius in the cutter head is approximately 300 to 350 mm for smaller TBMs, accommodating the assembly of 6–8-gauge cutters in this area. For larger TBMs (with

a radius exceeding 3 m), the transitional zone radius is around 600 to 650 mm, typically allowing for the assembly of 8–10 gauge cutters in this region.

The transitional zone radius must be adjusted to a reasonable value. If it is too small, the number of gauge cutters will decrease, leading to a reduced useful lifespan for the cutters. On the other hand, if it is excessively large, the cutter head's thickness will increase, resulting in a higher main load on the cutter head. Therefore, the transitional zone radius is a critical parameter in the optimal design of cutting tools for TBM. As a result, during the cutter head design process, the transitional zone is taken into account to determine the positioning of gauge cutters. Fig. 5 schematically depicts the transitional zone in the TBM cutter head.

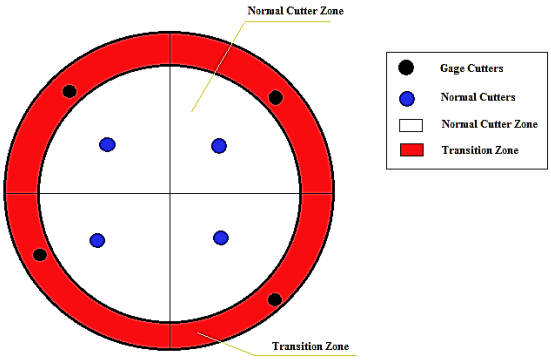

Fig. 5. Schematic of different cutter locations in the TBM cutter head.

2.2. Parametric Analysis Of The Cutter Tool Positions In The TBM Cutter-Head

To create and adapt an optimization model for the design of the cutter tool layout in the cutter head, it is essential to parametrically describe the positions of the cutter tools. By defining the parametric positions of the cutter tools within the cutter head, it is possible to formulate the equations, conditions, and constraints necessary to achieve an optimal design for the cutter tool layout. While Cartesian coordinate systems have been commonly used for representing point positions in various models, the circular geometry of the TBM cutter

head requires the utilization of a polar coordinate system for accurately describing the tool positions. In this system, the origin of the coordinate is the center of the cutter head, and the position of each cutter is defined based on the radial distance (ρ) and the trigonometric rotation angle (θ). Additionally, the cutter deviation angle (γ) is considered as a third parameter to determine the precise position of each cutter tool. By employing this coordinate system, the position of every cutter tool can be expressed using the following equation:

$$L_i = (\rho_i, \theta_i, \gamma_i)^T \in R^3 \qquad (1)$$

In Fig. 2, the position of the cutter is represented parametrically, considering the geometry of the cutter head and the defined coordinate system. The bounds of variation for each of the three parameters in Eq. (1) are as follows: Parameter ρ has values between zero and the radius of the cutter head, parameter θ has values between zero and 2π, and parameter γ has values between zero and π/2.

Based on the information provided, achieving the optimal positions for the cutting tools depends on finding the optimal values for the three parameters (ρ, θ, γ). Upon analyzing the normal and gauge cutters, it is evident that the deviation angle for the normal cutters is always zero. Consequently, when optimizing the positions of the normal cutters, only two parameters, ρ and θ, need to be optimized. On the other hand, for the gauge cutters, all three parameters will be considered in the evaluation process.

Additionally, considering the cutter placement zones, the ρ parameter values for the normal cutters range from zero to the boundary of the transitional zone. For the gauge cutters, this parameter encompasses the transitional zone and spans from the boundary of the transitional zone to the radius of the cutter head.

2.3. Spiral layout equations

The multi-spiral layout, depicted in Fig. 4, is commonly utilized for sequentially distributing cutters in the cutter head of medium and large-sized TBMs. This layout pattern is defined based on two parameters: the distance from the center (parameter ρ) and the trigonometric rotation angle (parameter θ).

To establish the equations governing the multi-spiral arrangement, 'n' is assumed as the total number of cutters, and 'm' as the number of spirals (based on the multi-spiral type, e.g., 2, 4, etc. - see Fig. 4). Consequently, the angular difference between two adjacent spirals is 2π/m. Assuming that 'j' is the counter of the cutters and targeting the position of the j-th cutter (ρ_j,θ_j), the equations are formulated as follows:

$$\text{if } \big(j > (m-1)\big)$$

$$\rho_j = (\rho_0 + i.\Delta p) + a\big(\theta_j + \theta_0\big) + i.\frac{2\pi}{m} \qquad (2)$$

$$i = \{0,1,\dots,m-1\}\,; \quad j = \{m,\dots,n-1\}$$

$$if\ \left(j \le (m-1)\right)$$
$$\theta_j = \theta_0 + \frac{2\pi}{m}.j \qquad (3)$$
$$j = \{0, 1, \dots, m-1)$$

In Eqs. (2) and (3), ρ_0 represents the radius (distance from the center) of the first normal cutter, Δp is the cutting spacing between the normal cutters, ' a ' is the shape coefficient, and θ_0 is the initial angle of the spiral layout. The Eq. (2) indicates that the angular position of the cutter, θ_j, is directly related to its radial distance, ρ_j. Additionally, ρ_j is determined based on the cutting spacing. Therefore, by defining the coefficients 'a' and the initial spiral angle, θ_0, the angular positions of the cutters, θ_j, can be determined. Consequently, with the knowledge of these two parameters (a, θ_0), the positions of the normal cutters in the multi-spiral layout can be formulated as shown in the following equation:

$$X_\theta = \{\theta_1, \theta_2, \dots, \theta_n\} = \{a, \theta_0\}$$
$$\theta_j = \begin{cases} \dfrac{\rho_j - (\rho_0 + i * \Delta p) - i * \frac{2\pi}{m}}{a} - \theta_0 & if\ (j > (m-1)) \\ \theta_0 + \dfrac{2\pi}{m} * j & if\ \ (j \le (m-1)) \end{cases} \qquad (4)$$
$$i = \{0,1, \dots, m-1\};\quad j = \{m, \dots, n-1\}$$

2.4. Star Layout Equations

Based on the star layout schematic presented in Fig. 5, it is evident that in this layout, the cutting tools are arranged on the cutter head face in a star-shaped pattern. Furthermore, the design requirements dictate that the gauge cutters are situated in the transitional zone, while the normal and center cutters are positioned outside the transitional zone on the cutter-head face (Fig. 5). The process of designing the star layout is based on predefining the number of star spokes. Initially, the type of star layout (e.g., 8-star, 12-star) is determined. Once the number of branches for the star layout is chosen, the entire circular cutter-head face is divided into a set of sections corresponding to the selected number of branches, thus forming a set for searching to find the optimal positions of the cutters.

For instance, when opting for an 8-star layout, the entire cutter-head face is divided into 8 equal sections. Subsequently, considering the parameter 'm' as the number of star branches, the search set (E) to determine the angular positions of the normal cutters is defined as follows:

$$E_i = i\ (2\pi/m) \qquad i = 1, 2, \dots, m \qquad (5)$$

Therefore, to find the optimal positions of the normal cutters, a search space for the distance from the center (parameter ρ) ranging from zero to the boundary of the transitional zone is considered. The rotation angle parameter (θ) is determined based on the search space E, which is computed using Eq. (5). The process of determining the optimal positions of the normal cutters is then carried out. The positions of the gauge cutters are determined using an infinite search space, where the parameter ρ represents the distance between the border of the transitional zone and the radius of the cutter head, and the parameter θ ranges from zero to 2π for positioning. With the provided explanation, the search space for obtaining the optimal positions of the normal and gauge cutters in the star layout is formulated as Eqs. (6) and (7) respectively:

$$\theta_i \in \{\theta \mid \theta = \theta_i + i\ (2\pi/m), i = 1, 2, \dots, m\ \} \qquad (6)$$
$$if\ \ \rho_i \in \{Normal\ cutter\ zone\}$$

$$\theta_i \in \{0, 2\pi\} \quad if\ \ \rho_i \in \{Transition\ zone\} \qquad (7)$$

2.5. Optimization Model

To achieve the optimal design for three layout types, namely stochastic, spiral, and star, taking into account all design requirements and constraints (Table 1), and utilizing the governing equations for the layout structure, a numerical optimization algorithm has been developed. The main optimization equation is divided into three separate parts, employing the GWO method to minimize it.

$$min\ y = f(X) = (C_1, C_2, C_3) \qquad (8)$$

Equation 8 involves three parameters: C_1, which corresponds to minimizing the forces eccentric forces; C_2, aimed at minimizing the eccentric torques; and C_3, focusing on eccentricity the cutting tools. These parameters are utilized to formulate the mechanical equations governing each of the functions C_1 to C_3, considering all the forces applied to the cutter.

- Definition of function C_1: Eccentric forces

$$C_1 = \sqrt{(\sum F_x)^2 + (\sum F_y)^2} \qquad (9)$$

In Eq. (9), the functions F_x and F_y represent the center cutters and normal cutters, respectively:

$$F_x = \sum_{i=1}^{Q} [F_{Ri}\ sin\ \theta_i + (F_{Si} + F_{ei})\ cos\ \theta_i] \qquad (10)$$

$$F_y = \sum_{i=1}^{Q} [-F_{Ri}\ cos\ \theta_i + (F_{Si} + F_{ei})\ sin\ \theta_i] \qquad (11)$$

In Eqs. (10) and (11), the parameter Q represents the number of cutters, F_R denotes the rolling force, F_S represents the lateral force, and F_e represents the inertial force of the cutter. The values of the lateral and the inertial forces are calculated using Eqs. (12) and (13), respectively:

$$F_{Si} = \frac{\tau}{2}(R\varphi)^2 \sin\left(\frac{R\varphi}{2\rho_i}\right) \quad (12)$$

$$F_{ei} = m\omega^2\rho_i \quad (13)$$

The parameters τ, m, and ω correspond to the shear strength of the rock, the cutter mass, and the rotational speed of the TBM cutter-head, respectively. The values of functions F_x and F_y for the gauge cutters are expressed using the following equations:

$$F_x = \sum_{i=1}^{Q}[F_{Ri}\sin\theta_i + F_{bi}\cos\theta_i] \quad (14)$$

$$F_y = \sum_{i=1}^{Q}[-F_{Ri}\cos\theta_i + F_{bi}\sin\theta_i] \quad (15)$$

I Eqs. (14) and (15), the parameter F_b denotes the impact of the cutter deviation angle (γ) on the applied force and is computed using the following equation:

$$F_{bi} = F_{ei} + F_{Si}\cos\gamma_i - F_{Ni}\sin\gamma_i \quad (16)$$

- Definition of function C_2: Eccentric torques

$$C_2 = \sqrt{(M_x)^2 + (M_y)^2} \quad (17)$$

In Eq. (17), M_x and M_y are defined for the cutters as follows in equations:

$$M_x = \sum_{i=1}^{Q}[-F_{Ni}\rho_i\sin\theta_i + M_i\sin\theta_i + F_{ei}r\sin\theta_i] \quad (18)$$

$$M_y = \sum_{i=1}^{Q}[-F_{Ni}\rho_i\cos\theta_i + M_i\cos\theta_i + F_{ei}r\cos\theta_i] \quad (19)$$

In Eqs. (18) and (19), the parameter M represents the cutter torque, which is calculated based on the following equation:

$$M_i = \frac{m\omega^2 r}{2}\rho_i \quad (20)$$

- Definition of function C_3: Eccentricity

$$C_3 = \sqrt{x_m^2 + y_m^2} \quad (21)$$

In Eq. (21), two parameters X_m and Y_m are formulated based on Eqs. (22) and (23).

$$x_m = \frac{\sum_{i=1}^{Q}\rho_i\cos\theta_i}{Q} \quad (22)$$

$$y_m = \frac{\sum_{i=1}^{Q}\rho_i\sin\theta_i}{Q} \quad (23)$$

2.5.1. Constraints Of Optimization Problem

Considering the design requirements and constraints (Table 1), the constraints of the optimization model for the optimal cutting tool layout design consist of four main constraints as follows:

- Constraint of non-overlapping positions of cutters

$$g_1(X) = \sum_{i=0}^{Q-1}\sum_{j=i+1}^{Q}\Delta V_{ij} \le 0 \quad (24)$$

In this equation, ΔV_{ij} represents the overlapping region between the positions of the i^{th} and j^{th} cutters.

- Constraint of consecutive cutting of adjacent cutters

$$g_2(X) = \sum_{i=0}^{Q-1}(\theta_{i+1} - \theta_i) \ge \Delta\theta \quad (25)$$

In this equation, the parameter Δ_θ represents the angular difference between two adjacent cutters.

- Constraint of static equilibrium (Constraint on the eccentricity of cutters)

$$g_3(X) = |x_m - x_e| - \delta x_e \le 0$$
$$g_4(X) = |y_m - y_e| - \delta y_e \le 0 \quad (26)$$

In this equation, O_m (X_m, Y_m) represents the actual center of the entire system, and O_e (X_e, Y_e) represents the desired expected position of O_m.

- Constraint of manholes and buckets' positions

$$g_5(X) = \{\forall i \in \{1, \dots, Q\}: C_i \cap OP \in \emptyset\} \quad (27)$$

This equation indicates that the cutters' positions are not located at the manholes, buckets positions.

2.6. Grey Wolf Optimization (GWO) Algorithm

The Grey Wolf Optimization (GWO) algorithm, introduced by Mirjalili et al. (2014), draws inspiration from the hunting behavior of a group of gray wolves. According to the hierarchy of wolves group life, the alpha (α) wolf, also known as the dominant wolf, is primarily responsible for making decisions about hunting, resting places, and movement timings.

The next level consists of the beta (β) gray wolves, who support the alphas in decision-making and other group activities. The beta (β) wolf is considered the most potential candidate to become the next alpha and acts as a deputy, fulfilling the role of an overseer for the pack.

The lowest level comprises the omega (ω) wolves. Omega wolves take on the role of victims or scapegoats within the pack, and they are the last ones to be allowed to eat. If a wolf does not fall into the categories of alpha, beta, or omega, it is known as a subordinate or delta (δ) wolf. Delta wolves obey the commands of alphas and betas, and they have authority over the omega wolves. The classification and hierarchical structure of grey wolves are illustrated in Fig. 6.

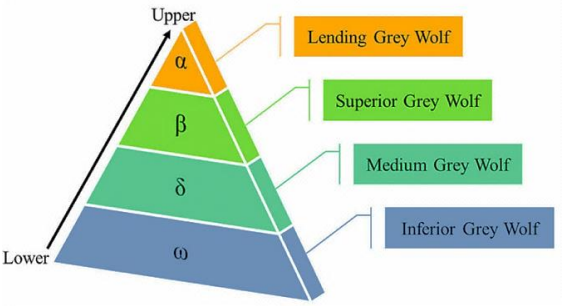

Fig. 6. Hierarchy of grey wolves (dominance and leadership decrease from top to bottom) (Mirjalili et al., 2014).

In the mathematical modeling of the social hierarchy of wolves during the design of the GWO algorithm, the most favorable solution is referred to as the alpha (α) wolf. Consequently, the second and third-best solutions are named after beta (β) and delta (δ) wolves, respectively. The remaining solutions are assumed to be omega (ω) wolves. In the GWO algorithm, optimization is driven by the alpha, beta, and delta wolves, while the omega wolves follow these three categories. Therefore, the GWO algorithm is inspired by the hunting process of grey wolves and involves three stages: 1) Search stage, 2) Siege stage, 3) Attack stage. These stages are formulated as follows:

2.6.1. Search Stage: Tracking, forcing to flee, and approaching the prey

The relationships presented for this search stage are as follows (Mirjalili et al., 2014):

$$\vec{D} = \left|\vec{C}.\overrightarrow{X_P}(t) - \vec{X}(t)\right|$$
$$\vec{X}(t+1) = \overrightarrow{X_P}(t) - \vec{A}\vec{D}| \quad (28)$$

This equation relates to the current iteration represented by parameter 't', where 'A' and 'C' are coefficient vectors. 'Xp' is the vector denoting the position of the prey, and 'X' represents the position vector of a grey wolf.

2.6.2. Siege Stage: Pursuing, encircling, and disrupting prey efficiency until it stops moving

$$\overrightarrow{D_\alpha} = \left|\overrightarrow{C_1}\,\overrightarrow{X_\alpha} - \vec{X}\right|$$
$$\overrightarrow{D_\beta} = \left|\overrightarrow{C_2}\,\overrightarrow{X_\beta} - \vec{X}\right| \quad (30)$$
$$\overrightarrow{D_\delta} = \left|\overrightarrow{C_3}\,\overrightarrow{X_\delta} - \vec{X}\right|$$

$$\overrightarrow{X_1} = \overrightarrow{X_\alpha} - \overrightarrow{A_1}.\left(\overrightarrow{D_\alpha}\right)$$
$$\overrightarrow{X_2} = \overrightarrow{X_\beta} - \overrightarrow{A_2}.\left(\overrightarrow{D_\beta}\right) \quad (31)$$
$$\overrightarrow{X_3} = \overrightarrow{X_\delta} - \overrightarrow{A_3}.\left(\overrightarrow{D_\delta}\right)$$

$$\bar{X}(t+1) = \frac{\bar{X}_1 + \bar{X}_2 + \bar{X}_3}{3} \quad (32)$$

Grey wolves possess the ability to identify the location of a prey and surround it. Hunting is usually guided by the alpha wolf. Beta and delta wolves may also participate in the hunting process under certain circumstances. However, in a constrained search space, there is no prior knowledge of the optimal location (prey). To mathematically simulate the hunting behavior of grey wolves, it is assumed that the alpha (the best solution), beta, and delta wolves have valuable information regarding the potential location of the prey.

As a result, the three best solutions obtained thus far are stored, compelling other search agents to update their positions based on the positions of these superior agents. The schematic representation of how the wolves update their positions in the hunting-siege stage is illustrated in Fig. 7.

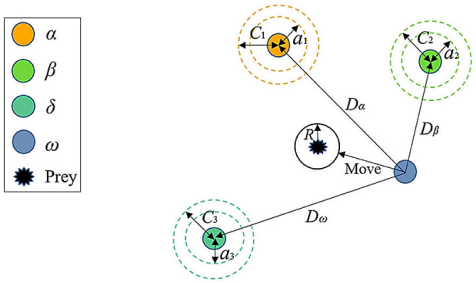

Fig. 7. Grey wolves' position vectors and updates.

2.6.3. Attack Stage: Initiation of the final attack towards the prey

Grey wolves conclude their hunting process by launching an attack on the prey when it stops moving. To achieve this, the implementation process decreases the value of the parameter 'a'. Moreover, the oscillation range of vector 'A' also decreases based on the value of 'a'. In other words, 'a' takes on a random value within the range -2a, 2a, where 'a' decreases from 2 to 0 as the number

of iterations increases. When the random values of 'A' fall within the range -1, 1, the next position of a search agent can lie anywhere between its current position and the position of the prey.

2.7. Algorithm for optimizing tool layout in numerical modeling

In this study, three distinct numerical models are developed to design optimal cutting tool layouts for cutter-head using three types of layouts: stochastic, spiral, and star patterns.

In the stochastic layout design model, the initial input data comprises two main parts: 1) TBM's initial specifications, and 2) the physical and mechanical properties of the hard rock (working face). Following this step, the main multi-objective optimization equation, along with the primary constraint equations, is formulated based on the provided relationships (Eqs. (8) to (27)). The primary design model for optimizing cutting tools in TBM is then established.

After adapting the model, the GWO algorithm is employed for optimization, resulting in the determination of the optimal positions for cutting tools (normal and gauge cutters). The algorithm's flowchart for the numerical optimization model of the optimal cutting tool layout with a stochastic layout is presented in Fig. 8.

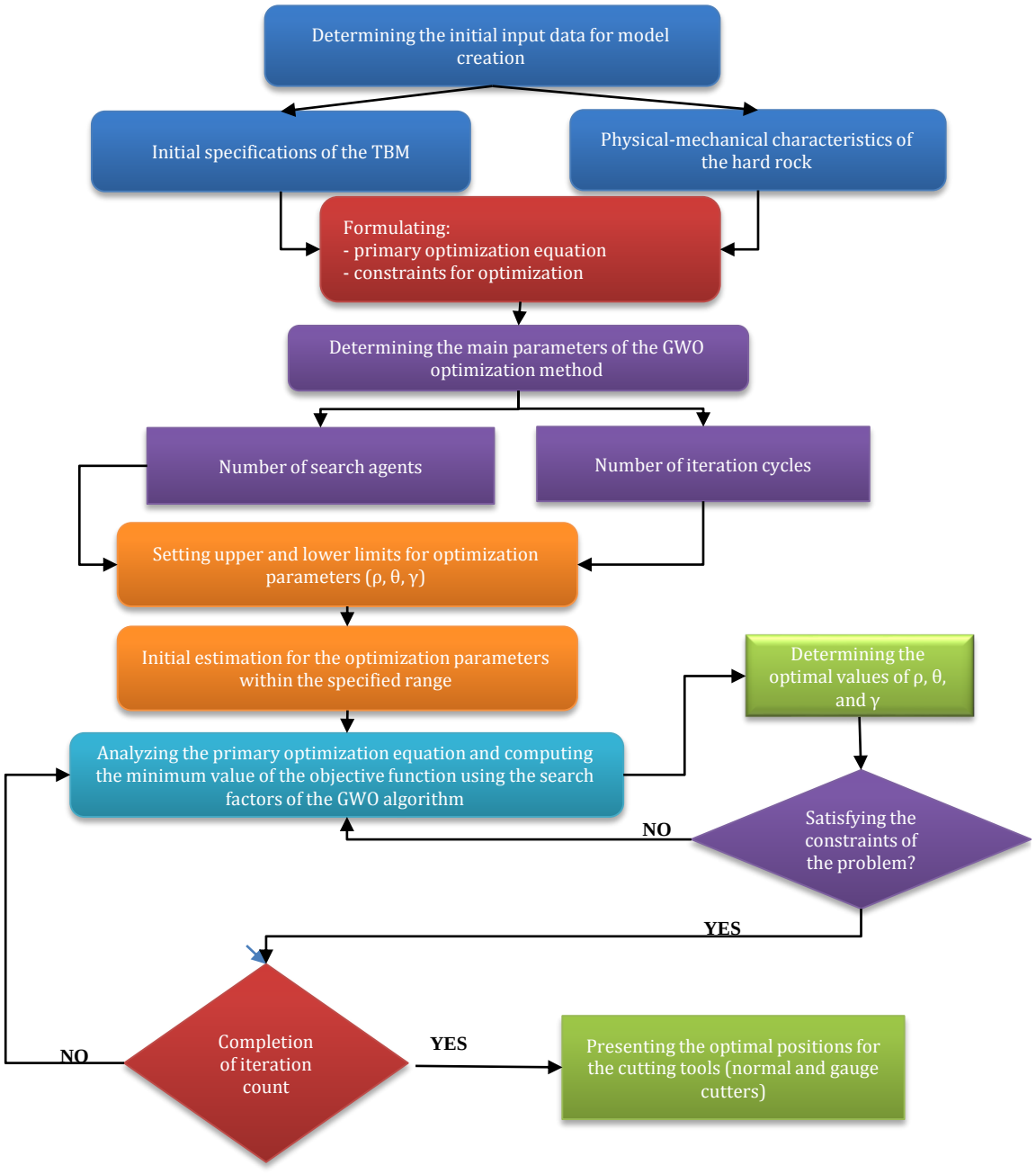

Fig. 8. An optimization model for the stochastic layout of the cutting tool based on the GWO algorithm.

In this study, a comprehensive numerical model is developed to optimize the spiral layout of cutting tools in TBM using the metaheuristic GWO algorithm. The input data for the model includes three main components: 1) TBM specifications, 2) physical and mechanical properties of the hard rock (working face), and 3) the type of spiral layout (2-spiral, 4-spiral, etc.).

Subsequently, the main multi-objective optimization equation, along with the primary constraint equations (Eqs. (26) and (27)), is formulated based on the provided relationships (Eqs. (8) to (23)).

The primary model for the optimal design of cutting tools in TBM is then adapted accordingly. It is important to note that in the spiral layout design model, two constraints of non-overlapping positions of cutters (Eq. (24)) and the constraint on the consecutive cutting of adjacent cutters (Eq. (25)) have been excluded from the equations of the spiral layout (Eqs. (2) to (4)). Therefore, these constraints are not considered optimization constraints in the model for the optimal design of the spiral cutting tool layout.

After adapting the model, the positions of cutters are initially determined by selecting values for two parameters (a, θ_0) based on the equations of the spiral layout (Eqs. (2) to (4)). Subsequently, the value of the main optimization equation (Eq. (8)) is calculated. Finally, utilizing the GWO algorithm, the optimization model is solved, and the optimal positions of the cutting tools within the spiral layout are computed and presented. The flowchart of the numerical algorithm for designing the optimal spiral cutting tool layout is depicted in Fig. 9. An optimal design model for the star layout of the cutting tool in the TBM cutter head has been developed based on design requirements, constraints, and the equations for the star layout. The numerical algorithm utilizes the GWO metaheuristic optimization method to achieve an efficient and effective solution.

According to the research model, the input data is divided into three main sections:

1- Specifications of the TBM,

2- Physical-mechanical characteristics of the hard rock (working face), and

3- The type of star layout (8-spoke, 12-spoke).

These input parameters are fed into the model for further optimization. Afterward, based on the provided equations (Eqs. (8) to (23)), the main multi-objective optimization equation is formulated, along with the primary constraint equations (Eqs. (24) to (27)), to establish the main optimization model for the optimal cutting tool layout in TBM. Once the model is set, by selecting values for two parameters (ρ, θ) within the defined search space, according to the equations of the star layout (Eqs. (5) to (7)), the positions of the cutters are determined. The value of the main optimization equation (Eq. (8)) is then calculated. Finally, utilizing the GWO algorithm, the optimization model is solved, and the optimal positions of the cutting tools within the star layout are computed and presented.

The numerical algorithm for designing the optimal positioning of cutting tools in a star layout is visually represented in the flowchart depicted in Fig. 10.

In the presented computational models for utilizing the GWO algorithm, the first step involves setting two initial parameters:

1- The number of search agents (number of wolves) and

2- The number of iterations in the calculations.

Subsequently, the GWO algorithm is applied to solve the optimization model. It is important to note that to satisfy the constraints and equations introduced under the optimization problem's constraints, a penalty technique is employed. In this approach, if any constraint is violated based on the values obtained for the optimization variables in each iteration of the model, a relatively large value is added to the objective function. Consequently, solutions that violate the problem's constraints are removed from the set of feasible solutions.

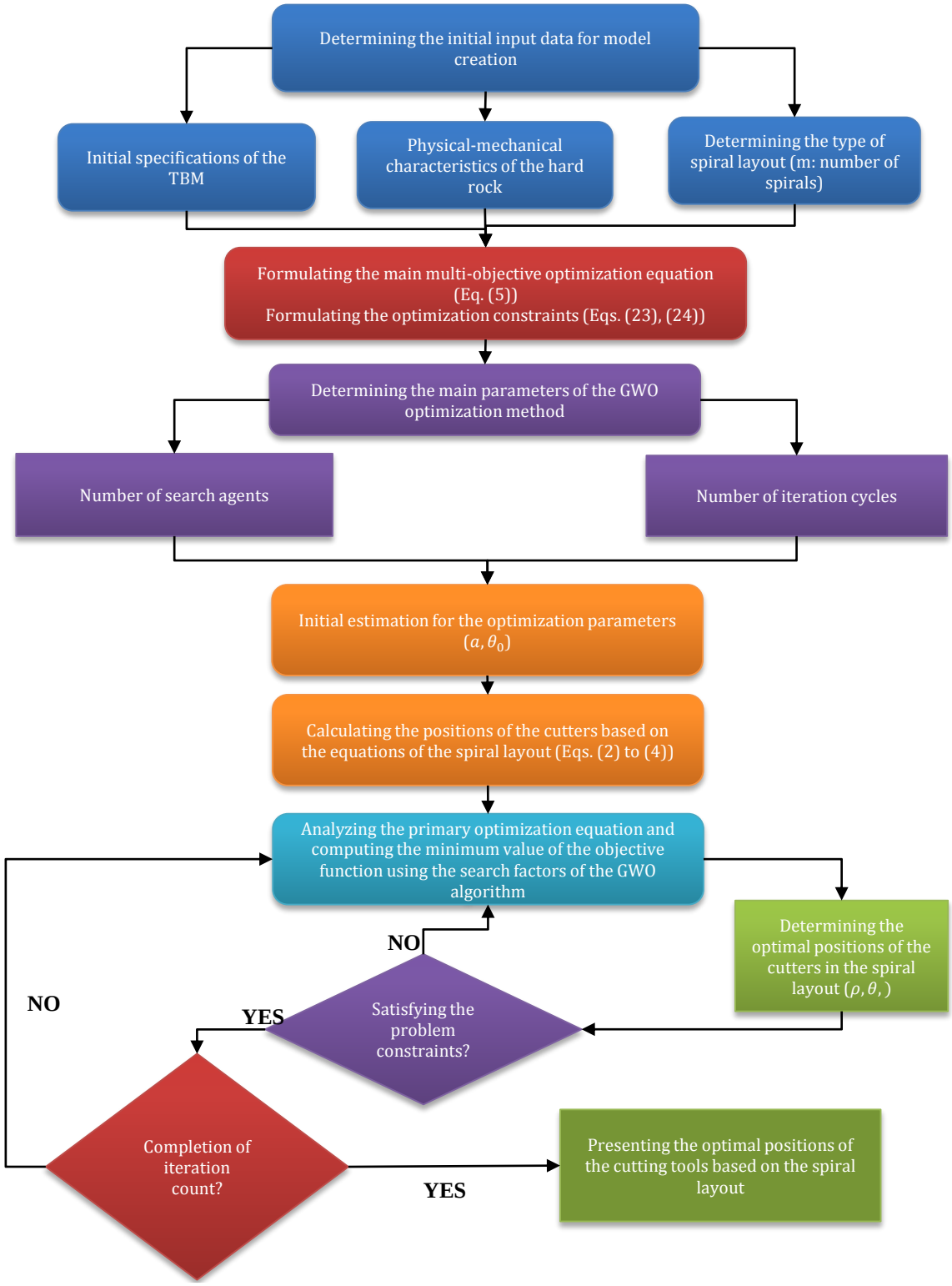

Fig. 9. An optimization model for the spiral layout of the cutting tool based on the GWO algorithm.

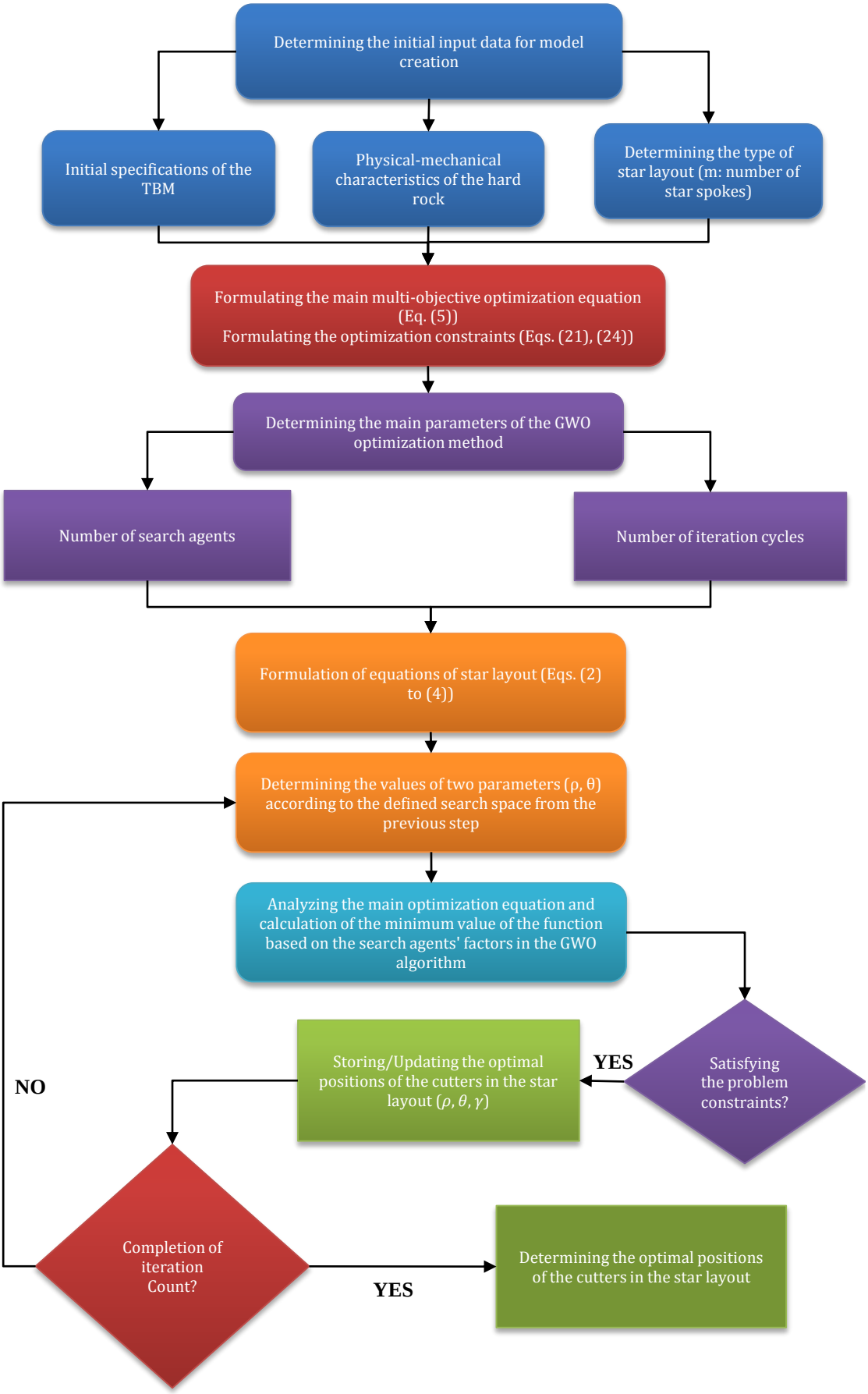

Fig. 10. Optimization model for star layout of cutting tool based on the GWO algorithm.

3. RESULTS AND DISCUSSION

To evaluate the performance of the optimization model, the process of designing the cutting tools layout in the cutter head was assessed using an executable TBM model. For this purpose, a hard rock TBM was employed for tunnel excavation in a water transfer project. The cutter-head consisted of 51-disc cutters (normal, gauge, and center cutters), based on engineering requirements. The study also considered 4 manholes and 8 buckets as part of the TBM system (Huo et al., 2010).

The TBM utilized in this investigation was equipped with four manholes, and their respective positions and geometric dimensions are presented in Table 2. Moreover, the TBM featured eight buckets, and their locations are detailed in Table 3. Additionally, Table 4 provides comprehensive information about various aspects, including the boring machine, cutting discs, and the physical characteristics of the rock.

Table 2. Manhole locations in the base TBM model (Huo et al., 2010)

Manhole number	1	2	3	4
ρ (mm)	2700	2700	2700	2700
θ (rad)	1.2217	2.793	4.363	5.934

Table 3. Dimensions and locations of buckets in the TBM model

Manhole number	ρ (mm)	θ (rad)	Length (mm)	Width (mm)
1	3700	0.611	700	300
2	3500	1.396	900	300
3	3700	2.182	700	300
4	3500	2.967	900	300
5	3700	3.753	700	300
6	3500	4.538	900	300
7	3700	5.323	700	300
8	3500	6.109	900	300

Table 4. Parameters of TBM and rock in the model

	Parameter	Value
Rock	Shear strength of rock punch (MPa)	7-13
	Uniaxial compressive strength (MPa)	50-93.6
	Tensile strength (MPa)	2.14-4
TBM	Cutter-head radius (m)	4.015
	Rotational speed (rad/s)	0.6283
	Mass of each cutter (kg)	200
	Cutter diameter (mm)	483
	Cutter width (mm)	10
	Cutter penetration (mm)	7
	Number of center cutters	8
	Number of normal cutters	33
	Number of gauge cutters	10
	Desired position for the center of the cutter head (x_e, y_e)	(0,0)
	Entire system eccentricity error value (mm) $\Delta x_e, \Delta y_e$	(5,5)
	Number of manholes	4
	Manhole radius	200
	Number of buckets	8

3.1. Results Obtained From Implementing The Model

Based on the presented numerical algorithms (Figs. 8 to 10), the optimization model for designing the optimal layout of three cutting tool layouts, namely stochastic, spiral, and star, has been implemented and developed in MATLAB software through coding.

The optimization model for designing the optimal layout of cutting tools and determining the best positions for normal and gauge cutters has been developed and presented using the GWO algorithm, taking into account the diverse characteristics and parameters introduced from the TBM model (Tables 2 to 4).

To calibrate the optimization model, in addition to the initial parameters of the machine and the physical characteristics of the hard rock, it is necessary to determine two parameters of the GWO algorithm: the number of search agents and the number of iterations. For this purpose, the number of search agents has been set to 30, and the number of iterations to 500. Subsequently, the optimization model is executed, and the optimal positions of the cutters are determined by minimizing the main equation (Eq. (8)) and satisfying the problem's constraints (Eqs. (24) to (27)) for three types of layouts: stochastic, spiral, and star (12 spokes).

In Fig. 11(a) to Fig. 11(c), the left-side plots illustrate the values obtained from the main optimization model as the number of iterations (optimization progress) increases for the stochastic, spiral, and star layouts, respectively. Upon completing the model execution and the optimization process, the optimal positions for the normal and gauge cutters were determined. The right side of Fig. 11 provides a schematic representation of the position of the cutting tools on the cutter-head for the three types of layouts.

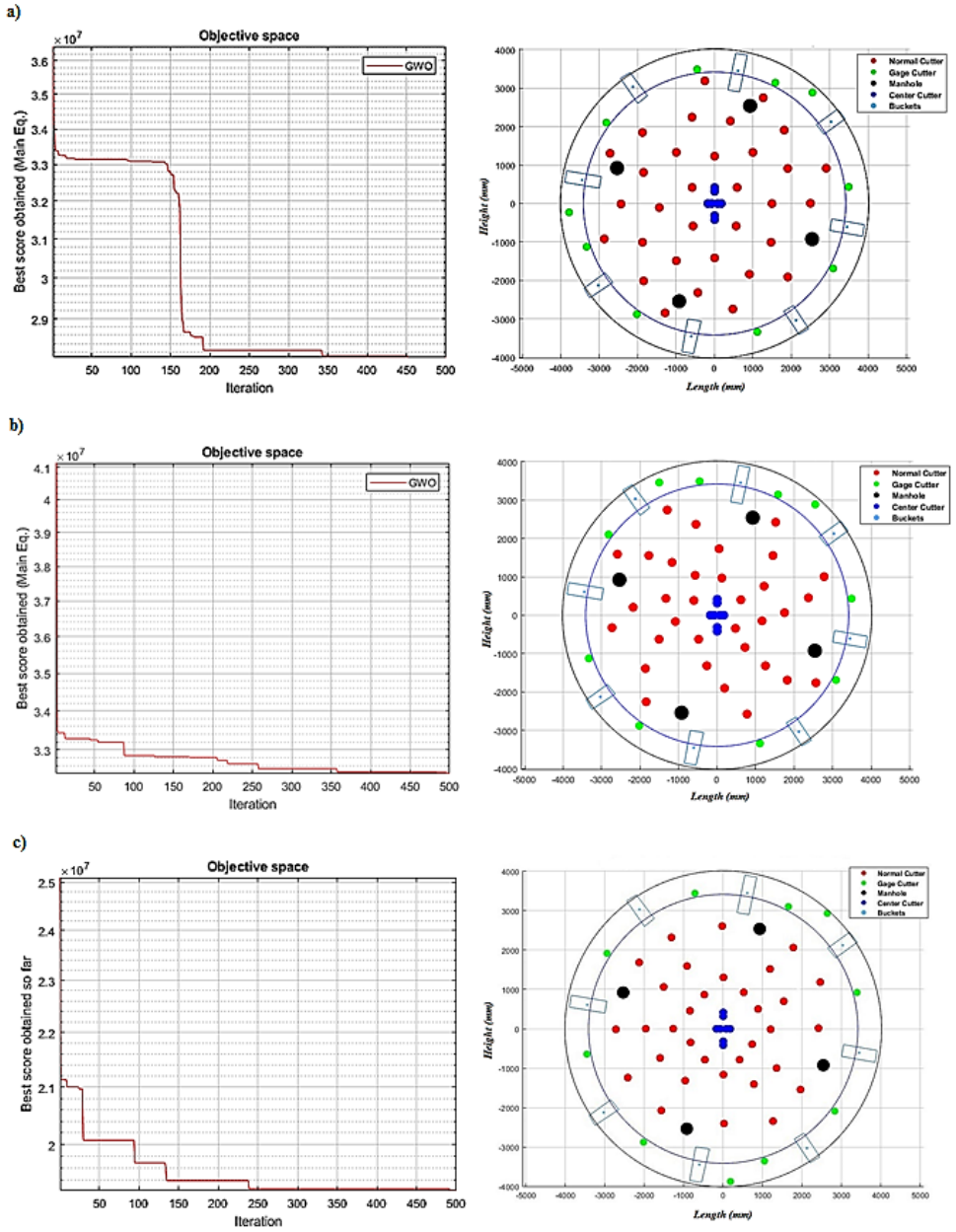

Fig. 11. Optimization process and schematic of cutting tool layout, a) Stochastic layout, b) Spiral layout, c) Star layout.

In Fig. 11 (left-side graphs), the optimization process based on the number of iterations of the GWO algorithm is presented for the main equation, considering three types of layouts: stochastic, spiral, and star. The results indicate that for the stochastic layout (Fig. 11(a)), the minimum computational values for the main equation decrease until iteration 350 and then remain constant. Similarly, for the spiral layout (Fig. 11(b)), the minimum computational values decrease until iteration 360 and then stabilize. Fig. 11(c) shows that the minimum values of the main equation decrease until iteration 240 and then remain constant. Based on these findings, choosing 500 iterations for the GWO optimization process for all three layouts, stochastic, spiral, and star (12-stokes), is deemed suitable.

Fig. 11(a) to Fig. 11(c) (on the right-hand side) illustrate the output of the numerical model for the optimized layouts of stochastic, spiral, and star. These graphs depict the optimal positions of the cutting tools on the TBM cutter head. The red circles represent the positions of the normal cutters, while the green circles represent the positions of the gauge cutters, as determined by the model's execution. Additionally, the positions of the center cutters are shown with blue circles, the positions of the Manholes are indicated with black circles, and the positions of the Buckets are displayed with turquoise rectangles.

3.2. Evaluation of the research model's performance

For the evaluation of the performance between the TBM and the three optimized layouts of stochastic, spiral, and star proposed in this research, compared to the original layout of the machine, four main parameters have been considered:

1) Total lateral force of the TBM

2) Eccentricity torques of the TBM

3) Assessment of the entire system eccentricity

4) Non-overlapping constraints of cutter positions and unsuccessful cuttings are compared and evaluated.

• Evaluation of the lateral force of the entire TBM (Parameter F_S)

$$F_S = \sum_{i=1}^{n} \overrightarrow{F_{Si}} \quad (33)$$

• Evaluation of the eccentricity torque of TBM (Parameter M_v)

$$M_V = \sum_{i=1}^{n} \overrightarrow{M_{Vi}} \quad (34)$$

In this equation, M_{vi} represents the eccentricity torque for the i^{th} cutter.

3.3. Evaluation Of Non-Overlapping Constraint Of Cutter Positions And Unsuccessful Cuttings

One of the crucial parameters in the analysis of the proposed layouts is the evaluation of non-overlapping of cutter positions. Considering the provided explanations, the evaluation has been carried out on four key parameters to compare the stochastic, spiral, and star layouts developed using the numerical models in this research with the original TBM cutter-head layout.

The results of the TBM performance evaluation based on the optimal stochastic, spiral, and star layouts are presented in Tables 5 to 7, respectively. It should be noted that the comparative values of the parameters for the original TBM layout are based on the data provided by the TBM manufacturer (Sun et al., 2018).

Table 5. Comparison of TBM performance based on the original cutting tools layout and the optimal stochastic layout

Parameter	Original Layout	Optimized layout	Percentage changes
Total lateral force F_s (KN)	154.840	8.4984	-146.35 (-94.57%)
Eccentric torque of the system M_v (KN.m)	11.558	7.4966	-4.0614 (-35.13%)
X_m eccentricity (mm)	-2.135	-0.064696	-2.0703 (-96.97%)
Y_m eccentricity (mm)	-0.221	0.17511	-0.3961 (-20.76%)
Overlap area of cutting tools positions	0.00	0.00	-
Number of cutters with unsuccessful cuttings	4	0	-4 (100%)

Table 5 displays a comparison of various performance parameters of the TBM between the original cutter-head layout and the optimized stochastic layout obtained from the research's optimization model. The results indicate that the total lateral force (F_s) of the optimal layout of cutting tools decreased by 146.35 KN, which accounts for a 94.57% reduction compared to the original layout. Furthermore, the amount of eccentric torque has decreased by 4.06 KN.m. Moreover, the eccentricity of the entire system (O (X_m, Y_m)) decreased by 2 mm for X_m and 0.39 mm for Y_m. The analysis of the provided data and the comparison of the obtained results reveal a remarkable improvement in the performance of the TBM when using the optimized cutting tools layout model as opposed to the original layout.

Table 6. Comparison of TBM performance based on the original cutting tools layout and the optimal spiral layout

Parameter	Original Layout	Optimized layout	Percentage changes
Total lateral force F_s (KN)	154.840	24.6589	-130.1811 (-84.07%)
Eccentric torque of the system M_v (KN.m)	11.558	9.12	-2.438 (-21.09%)
X_m eccentricity (mm)	-2.135	-0.98	-1.155 (-54.09%)
Y_m eccentricity (mm)	-0.221	-0.185	-0.036 (-16.28%)
Overlap area of cutting tools positions	0.00	0	-
Number of cutters with unsuccessful cuttings	4	0	-4 (100%)

Table 6 displays various performance parameters of the TBM based on the original cutting tools layout compared to the optimized spiral layout proposed by the developed optimization model in this research. The results indicate that the total lateral force on the TBM (F_s) has decreased by 130.18 KN compared to the original layout. Moreover, the eccentric torque has experienced a reduction of 2.438 KN.m, equivalent to 21.09% improvement. Additionally, the eccentricity (O (X_m, Y_m)) has reduced by 1.15 mm

for X_m and 0.036 mm for Y_m in the optimized layout.

Table 7. Comparison of TBM performance based on the original cutting tools layout and the optimal star layout

Parameter	Original Layout	Optimized layout	Percentage changes
Total lateral force F_s (KN)	154.840	18.7438	-136.09 (-87.89%)
Eccentric torque of the system M_v (KN.m)	11.558	8.82	-2.738 (-23.68%)
X_m eccentricity (mm)	-2.135	-0.72	-1.415 (-66.27%)
Y_m eccentricity (mm)	-0.221	-0.175	-0.046 (-20.81%)
Overlap area of cutting tools positions	0.00	0	-
Number of cutters with unsuccessful cuttings	4	0	-4 (100%)

Table 7 presents the results of comparing the performance of the star layout with the original TBM layout. According to the obtained results, the total lateral force (F_s) of the TBM decreased by 136.09 KN, equivalent to a substantial improvement of 87.89% in the optimized 12-spoke star layout compared to the original layout. Additionally, the eccentric torque was reduced by 2.738 KN.m. Moreover, the eccentricity values of the entire system (O (X_m, Y_m)) decreased by 1.415 mm for X_m and 0.046 mm for Y_m in the optimized star layout.

Based on the provided values and the comparison of the results (Tables 5 to 7), it is evident that the TBM's performance has significantly improved with the optimized layouts: stochastic, spiral, and star, as compared to the original TBM layout. To evaluate and compare the TBM's performance under these three cutting tool layouts, we have considered three key parameters: the total lateral force of the TBM, the eccentric torque of the TBM, and the overall system eccentricity. The results are presented in bar charts as shown in Fig. 12.

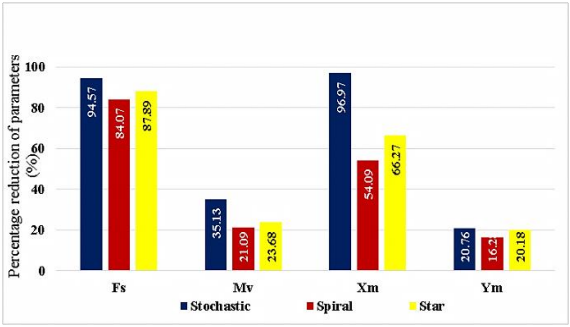

Fig. 12. Comparison of TBM performance based on stochastic, spiral, and star layouts.

Based on the results presented in the graphs of Fig. 12, it is evident that the TBM with the stochastic layout has exhibited superior performance compared to the spiral and star layouts. The total lateral force of the TBM has reduced by approximately 8% compared to the star layout and 10% compared to the spiral layout.

Additionally, the eccentric torque has decreased by 11% for the star layout and 14% for the spiral layout. Furthermore, the eccentricity parameter, X_m, has decreased by approximately 42% in the stochastic layout compared to the spiral layout and 30% compared to the star layout. Similarly, the eccentricity parameter, Y_m, has reduced by approximately 4% in the stochastic layout compared to the spiral layout and 1% compared to the star layout.

Based on the obtained results and the evaluation of TBM performance under the spiral and star layouts reveals that the TBM exhibited superior performance with the star layout compared to the spiral one. The star layout resulted in approximately 4% reduction in the total lateral force, 2.5% decrease in eccentric torque, around 12% reduction in the eccentricity parameter, X_m, and approximately 4% reduction in the eccentricity parameter, Y_m, compared to the spiral layout.

5. CONCLUSIONS

In this study, the performance of three different cutting tools layouts, stochastic, spiral, and star, in a mechanized TBM was evaluated through numerical modeling and implementation. In this regard, initially, three separate models have been developed for the optimal design of cutting tool layouts (based on technical engineering requirements and cutter-head structural requirements) in the TBM cutter-head. Furthermore, considering the equations for different layouts, three distinct models have been developed using the GWO algorithm to achieve optimal designs for stochastic, spiral, and star layouts of cutting tools in the TBM.

To evaluate the optimization model's performance and examine the effects of various layouts on the boring machine's performance, a TBM has been chosen. This TBM incorporates all the necessary geometric specifications, cutting details, cutters, equipment, and physical properties of the rock at the working face during drilling operations. The TBM's performance has been thoroughly assessed and compared under different conditions, including the original cutting tool layout and the optimal layouts of stochastic, spiral, and star layouts of cutting tools.

In this study, the performance of the TBM has been assessed using two different cutting tool

layouts: a 12-spokes star layout and a multi-spiral layout These layouts were compared to the original cutting tool layout to evaluate their respective designs and performances. The findings of this study reveal a remarkable enhancement in the performance of the TBM using the optimized models of stochastic, spiral, and star-cutting tool layouts compared to the original layout.

Based on the results, the lateral force on the entire machine, Fs, was reduced by 94.57%, 84.07%, and 87.89% for the stochastic, spiral, and star-optimized layouts, respectively, in comparison to the original cutting tool layout. Additionally, the eccentric torque decreased by 35.13%, 21.09%, and 23.68%, respectively, for the same layouts. Furthermore, the overall system eccentricity, O (X_m, Y_m), was reduced by 2.97 mm, equivalent to 96.97% for X_m, and by 0.39 mm, equivalent to 20.76% for Y_m in the case of the stochastic cutting tool layout. The parameter values for the eccentricity in the spiral and star-cutting tool layouts are 1.15 and 1.41 mm for X_m, and 0.036 and 0.046 mm for Y_m, respectively. These values indicate a reduction compared to the original cutting tool layout.

The comparison of results obtained from the performance of the TBM with stochastic, spiral, and star-cutting tool layouts reveals that the TBM with the stochastic layout has exhibited superior performance compared to the spiral and star layouts. The overall lateral force on the machine decreased by approximately 8% compared to the star layout and 10% compared to the spiral layout. Additionally, the eccentric torque was reduced by about 11% compared to the star layout and 14% compared to the spiral layout. Furthermore, the X_m parameter for the eccentricity in the stochastic layout decreased by roughly 42% compared to the spiral layout and 30% compared to the star layout. Similarly, the Y_m parameter for the eccentricity decreased by approximately 4% compared to the spiral layout and 1% compared to the star layout.

According to the results and performance evaluation of the TBM under the spiral and star cutting tool layouts, it is evident that the TBM with the star layout has shown better performance compared to the spiral layout. The star layout resulted in a reduction of approximately 4% in the overall lateral force on the machine, 2.5% in the eccentric torque, about 12% in the X_m parameter for the eccentricity, and approximately 4% in the Y_m parameter for the eccentricity compared to the spiral layout.

The most significant achievement of this research is the development of a comprehensive and efficient model for designing optimal cutting tool layouts (stochastic, spiral, and star) in TBMs using the GWO algorithm. This model can be applied under various operational conditions and is suitable for different types of TBMs. Utilizing initial data, such as the physical properties of the hard rock, cutting tool characteristics, and cutting geometry, the model can generate three types of optimal layouts for cutting tools in the TBM. This model holds great potential for widespread use by professionals and designers in the field of mechanized drilling.

REFERENCES

[1] Abu Bakar, M.Z., Gertsch, L.S. Rostami, J., 2014. Evaluation of fragments from disc cutting of dry and saturated sandstone. Rock Mechanics and Rock Engineering, 47, 1891-1903.

[2] Alber, M., Yaralı, O., Dahl, F., Bruland, A., Käsling, H., Michalakopoulos, T.N., Cardu, M., Hagan, P., Aydın, H. Özarslan, A., 2015. ISRM suggested a method for determining the abrasivity of rock by the CERCHAR abrasivity test. The ISRM suggested methods for rock characterization, testing, and monitoring: 2007-2014, 101-106.

[3] Bruland, A., 2000. Hard rock tunnel boring. PhD Thesis, Norwegian University of Science and Technology, Trondheim, Norway.

[4] Cardu, M., Iabichino, G., Oreste, P. Rispoli, A., 2017. Experimental and analytical studies of the parameters influencing the action of TBM disc tools in tunneling. Acta Geotechnica, 12(2), 293-304.

[5] Cho, J.W., Yu, S.H., Jeon, S.W., Chang, S.H., 2008. Numerical study on rock fragmentation by TBM disc cutter. Journal of Korean Tunnelling and Underground Space Association, 10(2), 139-152.

[6] Choi, S.O., Lee, S.J., 2015. Three-dimensional numerical analysis of the rock-cutting behavior of a disc cutter using particle flow code. KSCE Journal of Civil Engineering, 19, 1129-1138.

[7] Cigla, M., Yagiz, S., Ozdemir, L., 2001, June. Application of tunnel boring machines in underground mine development. In 17th international mining congress and exhibition of Turkey, Ankara, 155-164.

[8] Duan, W., Zhang, L., Zhang, M., Su, Y., Mo, J. Zhou, Z., 2022. Numerical and experimental studies on the effects of the TBM cutter profile on rock cutting. KSCE Journal of Civil Engineering, 26, 416-432.

[9] Emmanuel, D.A.D.A., Joseph, S., Oyewola, D., Fadele, A.A., Chiroma, H., 2021. Application of grey wolf optimization algorithm: Recent trends, issues, and possible horizons. Gazi University Journal of Science, 35(2), 485-504.

[10] Farrokh, E., 2021. Layout design specifications of hard-rock TBM cutter heads at maximum cutter

penetration and TBM advance. Arabian Journal of Geosciences, 14(19), 2049.

[11] Farrokh, E., 2022. Lace Design Optimization for Hard Rock TBMs. Amirkabir Journal of Civil Engineering, 53(12), 5517-5534.

[12] Geng, Q., Bruland, A., Macias, F.J., 2018. Analysis of the relationship between layout and consumption of face cutters on hard rock tunnel boring machines (TBMs). Rock Mechanics and Rock Engineering, 51, 279-297.

[13] Gong, Q.M., Zhao, J., Hefny, A.M., 2006a. Numerical simulation of rock fragmentation process induced by two TBM cutters and cutter spacing optimization. Tunnelling and Underground Space Technology incorporating Trenchless Technology Research, 21(3), 263-263.

[14] Gong, Q.M., Jiao, Y.Y., Zhao, J., 2006b. Numerical modeling of the effects of joint spacing on rock fragmentation by TBM cutters. Tunnelling and Underground Space Technology, 21(1), 46-55.

[15] Gong, Q.M., Zhao, J., Jiao, Y.Y., 2005. Numerical modeling of the effects of joint orientation on rock fragmentation by TBM cutters. Tunneling and underground space technology, 20(2), 183-191.

[16] Huo, J., Sun, W., Chen, J., Zhang, X., 2011. Disc cutters plane layout design of the full-face rock tunnel boring machine (TBM) based on different layout patterns. Computers & Industrial Engineering, 61(4), 1209-1225.

[17] Huo, J., Sun, W., Chen, J., Su, P., Deng, L., 2010. Optimal disc cutters plane layout design of the full-face rock tunnel boring machine (TBM) based on a multi-objective genetic algorithm. Journal of Mechanical Science and Technology, 24, 521-528.

[18] Huo, J., Wu, H., Yang, J., Sun, W., Li, G., Sun, X., 2015. Multi-directional coupling dynamic characteristics analysis of TBM cutter head system based on tunneling field test. Journal of Mechanical Science and Technology, 29, 3043-3058.

[19] Huo, J., Sun, W., Chen, J., Zhang, X., 2011b. Disc cutters plane layout design of the full-face rock tunnel boring machine (TBM) based on different layout patterns. Computers & industrial engineering, 61(4), 1209-1225.

[20] Jeong, H.Y., Jeon, S.W., Cho, J.W., Chang, S.H., Bae, G.J., 2011. Assessment of cutting performance of a TBM disc cutter for anisotropic rock by linear cutting test. Tunnel and Underground Space, 21(6), 508-517.

[21] Liang, Q., Zhang, D., Coppola, G., Mao, J., Sun, W., Wang, Y., Ge, Y., 2016. Design and analysis of a sensor system for cutting force measurement in machining processes. Sensors, 16(1) 70.

[22] Liu, W., Li, A., Liu, C., 2022. Multi-objective optimization control for tunnel boring machine performance improvement under uncertainty. Automation in Construction, 139, 104310.

[23] Lin, L., Xia, Y., Wu, D., 2019. Multiobjective optimization design for structural parameters of TBM disc cutter rings based on FAHP and sampga. Advances in Civil Engineering, 2019.

[24] Macias, F.J., 2016. Hard rock tunnel boring: performance predictions and cutter life assessments. PhD Thesis, Norwegian University of Science and Technology, Trondheim, Norway.

[25] Macias, F.J., Wilfing, L., Andersson, T., Thuro, K., Bruland, A., 2015, October. Performance and cutter life assessments in hard rock tunneling. In ISRM EUROCK. ISRM.

[26] Mazaira, A., Konicek, P., 2015. Intense rockburst impacts in deep underground construction and their prevention. Canadian Geotechnical Journal, 52(10), 1426-1439.

[27] Mirjalili, S., Mirjalili, S.M., Lewis, A., 2014. Grey wolf optimizer. Advances in engineering software, 69, 46-61.

[28] Moon, T., 2005. A computational methodology for modeling rock cutting with a discrete element method: Prediction of TBM rock cutting performance. PhD Thesis, Colorado, Colorado School of Mines.

[29] Rostami, J., 2008. Hard rock TBM cutter head modeling for design and performance prediction. Geomechanik und Tunnelbau: Geomechanik und Tunnelbau, 1(1), 18-28.

[30] Sun, H.Y., Guo, W., Liu, J.Q., Song, L.W., Liu, X.Q., 2018. Layout design for disc cutters based on analysis of TBM cutter-head structure. Journal of Central South University, 25(4), 812-830.

[31] Sun, W., Ling, J., Huo, J., Guo, L., Zhang, X., Deng, L., 2013. Dynamic characteristics study with multidegree-of-freedom coupling in TBM cutter head system based on complex factors. Mathematical Problems in Engineering, 2013.

[32] Wang, L., Kang, Y., Zhao, X., Zhang, Q., 2015. Disc cutter wear prediction for a hard rock TBM cutter head based on energy analysis. Tunnelling and Underground Space Technology, 50, 324-333.

[33] Yang, M., Xia, Y.M., Lin, L.K., Qiao, S., Ji, Z.Y., 2020. Optimal design for buckets layout based on muck removal analysis of TBM cutter head. Journal of Central South University, 27(6), 1729-1741.

[34] Yu, S.H., 2007. A study on rock cutting behavior by TBM disc cutter. MSc Thesis, Seoul National University, Seoul, Korea.

[35] Zhang, P., 2009. Design and research on cutter layout and the structural parameters of the cutter head optimization for TBM.

[36] Zhao-Huang, Z. and Yong-Li, Q. (2011), "Research on the layout of TBM disc cutter", Engineering Mechanics, 28(5), 172-177.